

Metal-insulator transition and local-moment collapse in FeO under pressure

I. Leonov

*Theoretical Physics III, Center for Electronic Correlations and Magnetism,
Institute of Physics, University of Augsburg, 86135 Augsburg, Germany*

(Dated: June 19, 2021)

We employ a combination of the *ab initio* band structure methods and dynamical mean-field theory to determine the electronic structure and phase stability of paramagnetic FeO at high pressure and temperature. Our results reveal a high-spin to low-spin transition within the B1 crystal structure of FeO upon compression of the lattice volume above 73 GPa. The spin-state transition is accompanied by an orbital-selective Mott metal-insulator transition (MIT). The lattice volume is found to collapse by about 8.5 % at the MIT, implying a complex interplay between electronic and lattice degrees of freedom. Our results for the electronic structure and lattice properties are in overall good agreement with experimental data.

PACS numbers: 71.10.-w, 71.27.+a, 71.30.+h

I. INTRODUCTION

Iron monoxide, wüstite (FeO), is a basic oxide component of the Earth's interior. Its electronic state and phase stability is of fundamental importance for understanding the properties and evolution of the Earth's lower mantle and outer core.¹ Nevertheless, in spite of long-term intensive research, the phase diagram of FeO at high pressures and temperatures, as well as several key properties, such as electronic structure and magnetic properties, are still poorly understood.

FeO has a relatively complex pressure-temperature phase diagram with at least five allotrops.¹ Under ambient conditions, it is a paramagnetic Mott insulator with a rock-salt B1 crystal structure. Upon compression above ~ 16 GPa, B1-type FeO undergoes a structural transition to the rhombohedral $R\bar{3}$ phase (rB1),³ which further transforms to the NiAs (B8) structure above 90 GPa.⁴ Under ambient pressure, FeO is antiferromagnetic below the Néel temperature $T_N \sim 198$ K.² The high-pressure properties of FeO have attracted much recent interest both from a theoretical and experimental point of views.^{6–15} Shock-wave compression and electrical conductivity experiments reported a possible existence of a high-pressure metallic phase of FeO above ~ 70 GPa.¹⁶ On the basis of high-pressure Mössbauer spectroscopy measurements,¹⁷ the metallic state was assigned to a high-spin (HS) to low-spin (LS) transition, which has been proposed by first-principles calculations to occur above ~ 100 -200 GPa.⁶ In contrast to that, x-ray emission spectroscopy indicates that the Fe high-spin state is preserved at least up to ~ 140 GPa (at room temperature),¹⁸ while collapsing to the LS state upon further heating.¹⁹ On the basis of these measurements, the insulator-to-metal HS-LS transition has long been considered to be due to a structural transformation from the B1 to B8 lattice. Nevertheless, recent experiments have shown that the B1-type FeO undergoes a high-temperature insulator-to-metal transition at about 70 GPa, retaining the same lattice structure.¹⁴ The observed metallic phase was proposed to relate to a spin-

state crossover. Moreover, it has been shown that the B1-type structure remains stable at high pressure and temperature, being the stable phase along the geotherm through the Earth's mantle and outer core.^{1,20}

These recent experiments have lead us to reinvestigate the electronic structure and local magnetic state of Fe in FeO at high pressure and temperature by employing a combination of the *ab initio* electronic structure methods and dynamical mean-field theory of strongly correlated electrons (LDA+DMFT).^{21,22} (LDA stands here for the local density approximation). Applications of LDA+DMFT have shown to capture all generic aspects of a Mott metal-insulator transition, such as a coherent quasiparticle behavior, formation of the lower- and upper-Hubbard bands, and strong renormalization of the effective electron mass, providing a good quantitative description of the electronic and lattice properties. In particular, we employ an important advance of the LDA+DMFT approach which is able to determine the electronic structure and phase stability of correlated materials.^{23–38} We use this advanced theory to investigate the electronic structure and phase stability of paramagnetic FeO at high pressure and temperature, which remained unexplored up to now. We find that magnetic collapse occurs in the B1 crystal structure of paramagnetic FeO upon compression to ~ 73 GPa, in agreement with experiment. The HS-LS transition is intimately linked with an orbital-selective Mott metal-insulator transition, which is accompanied with a collapse of the lattice volume by about 8.5 % at the MIT. Our results for the electronic structure and lattice properties are in overall good agreement with experimental data.

II. METHOD

In this work, we investigate the electronic structure and phase stability of paramagnetic FeO under pressure using the GGA+DMFT computational approach (GGA: generalized gradient approximation). To this end,

we calculate the total energy and local moments of the B1 cubic crystal structure of FeO as a function of lattice volume. Below we denote the compressed phase by the relative volume w.r.t. the calculated equilibrium lattice volume as $\nu \equiv V/V_0$. We employ a fully charge self-consistent GGA+DMFT approach³⁹ implemented with plane-wave pseudopotentials⁴⁰. For the partially filled Fe 3d and O 2p orbitals we construct a basis set of atomic-centered symmetry-constrained Wannier functions^{41,42}. To solve the realistic many-body problem, we employ the continuous-time hybridization-expansion quantum Monte-Carlo algorithm⁴³. The calculations are performed in the paramagnetic state at temperature $T = 1160$ K. We use the average Coulomb interaction $U = 7$ eV and Hund's exchange $J = 0.89$ eV for the Fe 3d shell, in accordance with previous estimates^{7,10,13,14}. The Coulomb interaction is treated in the density-density approximation. The spin-orbit coupling is neglected in these calculations. The U and J values are assumed to remain constant upon variation of the lattice volume. In addition, we check how our results depend on a possible reduction of the U value under pressure. For this purpose, we perform calculations with a substantially smaller value, $U = 5$ eV. We employ the fully-localized double-counting correction, evaluated from the self-consistently determined local occupancies, to account for the electronic interactions already described by GGA. The spectral functions were computed using the maximum entropy method. The angle resolved spectra were evaluated from analytic continuation of the self-energy using Padé approximants.

III. RESULTS AND DISCUSSION

We first compute the electronic structure of FeO within non-spin-polarized GGA using the plane-wave pseudopotential approach.⁴⁰ Overall, our results agree well with previous band-structure calculations. In particular, the calculated equilibrium lattice constant is found to be $a = 7.74$ a.u. The calculated bulk modulus is $B = 232$ GPa. We note however that GGA calculations give a metallic solution, in qualitative disagreement with experiment. The calculated equilibrium lattice constant is remarkably smaller, by ~ 6 -7 %, than the experimental one. We also note a strong overestimation of the bulk modulus, which is more than ~ 25 % off the experimental value. Clearly, standard band-structure techniques cannot explain the properties of paramagnetic FeO, since they do not treat electronic correlations adequately.

To resolve this obstacle, we now compute the electronic structure and phase stability of FeO using the fully charge self-consistent GGA+DMFT method. In Fig. 1 (top) we show the evolution of the total energy and local magnetic moment $\sqrt{\langle m_z^2 \rangle}$ of paramagnetic FeO as a function of lattice volume. We fit the calculated total energy using the third-order Birch-Murnaghan equation of states⁴⁵ separately for the low- and high-volume regions. Overall, our

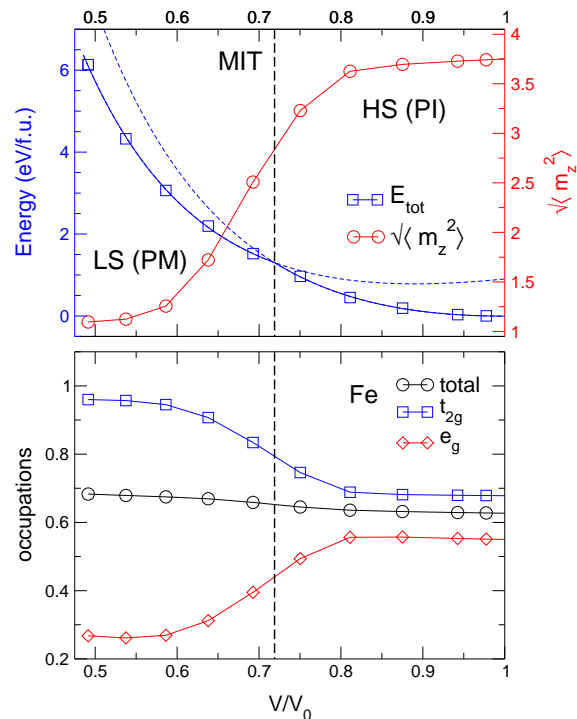


FIG. 1: Top: Total energy and local moment $\sqrt{\langle m_z^2 \rangle}$ of paramagnetic FeO calculated by GGA+DMFT as a function of lattice volume. The lattice collapse associated with the HS-LS state transition is depicted by a vertical black dashed line. Bottom: Fe 3d and partial t_{2g}/e_g occupancies as a function of volume.

results for the electronic structure and lattice properties of FeO, which now include the effect of electronic correlations, agree well with experimental data. In particular, our calculations at ambient pressure give a Mott insulating solution with an energy gap of ~ 0.8 eV. The energy gap lies between the top of the valence band originating from the mixed Fe 3d and O 2p states and empty Fe 4s states. Our result for the Mott d - d energy gap is about 2 eV, in good agreement with optical and photoemission experiments.⁴⁴ We find the equilibrium lattice constant $a = 8.36$ a.u., which is less than 1-2 % off the experimental value. The calculated bulk modulus is $B = 140$ GPa, the local magnetic moment $\sqrt{\langle m_z^2 \rangle} \sim 3.7 \mu_B$. Fe t_{2g} and e_g orbital occupancies are 0.68 and 0.55, respectively. These findings clearly indicate that at ambient pressure Fe²⁺ ion is in a high-spin state ($S = 2$). In fact, in a cubic crystal field, the Fe²⁺ ions (i.e., Fe 3d⁶ configuration with four electrons in the t_{2g} and two in the e_g orbitals) have a local moment of $4 \mu_B$.

Furthermore, the total-energy and local-moment calculation results exhibit a remarkable anomaly upon compression of the lattice volume down to $\nu \sim 0.72$. Indeed, the local moment is seen to retain its high-spin value down to about $\nu \sim 0.8$. Upon further compression, a broad high-spin (HS) to low-spin (LS) crossover takes place, with a collapse of the local moment to a

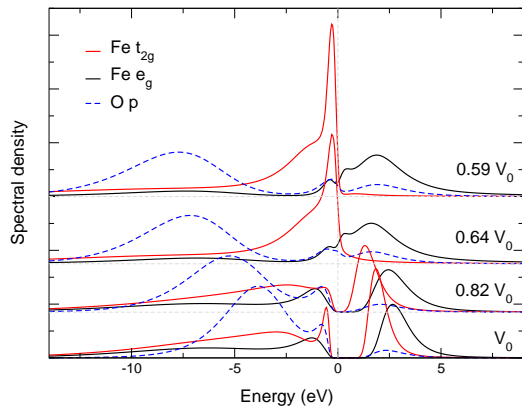


FIG. 2: Evolution of the spectral function of paramagnetic FeO as a function of lattice volume. Fe t_{2g}/e_g and O p orbital contributions are shown. The metal-insulator transition associated with the HS-LS transformation takes place at $\nu \sim 0.72$, at pressure ~ 73 GPa.

LS state with magnetic moment $\sim 1.2 \mu_B$ at pressure above 160 GPa, i.e., $\nu < 0.6$. We display our results for the evolution of the Fe t_{2g} and e_g orbital occupations in Fig. 1 (bottom). Upon compression, we observe a substantial redistribution of charge between the t_{2g} and e_g orbitals within the Fe $3d$ shell. Fe t_{2g} orbital occupations are found to gradually increase with pressure, resulting in (almost) completely occupied state (t_{2g} occupation is about 0.95). On the other hand, the e_g orbitals are strongly depopulated (their occupation is 0.25) and the Fe $3d$ total occupancy remains essentially unchanged with pressure. We therefore interpret this spin crossover as a HS-LS transition.

The spin-state transition is accompanied by a structural transformation. The structural change takes place upon a compression of the lattice volume to $\nu \sim 0.72$, resulting in a collapse of the lattice volume by $\sim 8.5\%$. This value should be considered as an upper-bound estimate because we neglect multiple intermediate-phase transitions when fit the total-energy result to the third-order Birch-Murnaghan equation of states. Our estimate for the transition pressure is $p = 73$ GPa. In addition, we note that the bulk modulus in the HS phase is somewhat smaller than that in the LS phase (162 GPa), implying an enhancement of the compressibility at the phase transition. Overall, the electronic structure, the equilibrium lattice constant, and the structural phase stability of paramagnetic FeO obtained by the fully charge self-consistent GGA+DMFT approach are in remarkably good agreement with the experimental data. Our findings clearly indicate the crucial importance of electronic correlations to explain the electronic structure and lattice properties of paramagnetic FeO.

Next we address the spectral properties of paramagnetic FeO. In Fig. 2 we present the evolution of the spectral function of FeO as a function of lattice volume. We note that at ambient pressure paramagnetic

FeO is a Mott insulator with a relatively large $d-d$ gap ~ 2 eV. Interestingly, the energy gap lies between the Fe t_{2g} states, while the $t_{2g}-e_g$ gap is somewhat larger, ~ 2.5 eV. The top of the valence band has a mixed Fe $3d$ and O $2p$ character, with a resonant peak in the filled t_{2g} band located at about -0.9 eV. The latter can be ascribed to the formation of a Zhang-Rice bound state.⁴⁶ We find the $d-d$ energy gap being gradually decreased upon compression, resulting in an orbital-selective Mott metal-insulator transition (MIT). In fact, the onset of the local moment collapse at $\nu \sim 0.75$ is associated with closing of the gap for the t_{2g} orbitals, while the e_g states remain to be gaped down to $\nu \sim 0.7$. We note that the HS-LS transition takes place upon compression of the lattice volume by $\nu \sim 0.72$, at critical pressure of $p \sim 73$ GPa, in agreement with experiment. Our calculations clearly show that the HS-LS state transition in the B1 structure of paramagnetic FeO is associated with an orbital-selective Mott-Hubbard MIT. Moreover, the MIT is accompanied by a collapse of the lattice volume by about 8.5% .

In addition, we check how the electronic structure of FeO depend on a (possible) reduction of the Coulomb interaction U with pressure. For this purpose, we perform calculations with a substantially smaller value $U = 5$ eV and the same Hund's coupling value $J = 0.89$ eV. Our new results are in overall qualitative agreement with those presented above. We notice that the HS-LS crossover is accompanied by an orbital-selective MIT which is found to occur at somewhat smaller compression $\nu \sim 0.77$, at critical pressure 55 GPa. We also note a substantial reduction of the Mott $d-d$ band gap to about 1.1 eV, whereas the charge-transfer gap between the Fe $3d$ -O $2p$ and empty Fe $4s$ states remains unchanged, about 0.8 eV. These findings clearly indicate that our results for the spin-state crossover and associated with it the orbital-selective MIT are robust. The HS to LS transition takes place even at a substantially reduced (possibly due to the applied pressure) value of U .

We also calculated the momentum-resolved spectral function of paramagnetic FeO. In Fig. 3 we present our results obtained for the B1 structure of paramagnetic FeO across the MIT. Our calculations at ambient pressure show a Mott insulator with an energy gap value of ~ 0.8 eV [see Fig. 3 (bottom)]. The energy gap lies between the occupied states with a mixed Fe $3d$ -O p character and empty Fe $4s$ state (the latter is clearly seen as a broad parabolic-like band at the Γ -point just above the Fermi energy), in agreement with photoemission and optical experiments.⁴⁴ In fact, the optical spectroscopy measurements observe a weak absorption between 0.5 and 2.0 eV, assigned to the Fe $3d$ -O $2p$ to Fe $4s$ transitions. The strong absorption edge associated with the $d-d$ transitions is found to appear in optical spectroscopy at about 2.4 eV. Our result for the $d-d$ gap at ambient pressure is about 2 and 2.5 eV for the $t_{2g}-t_{2g}$ and $t_{2g}-e_g$ transitions, respectively. The O $2p$ states are about

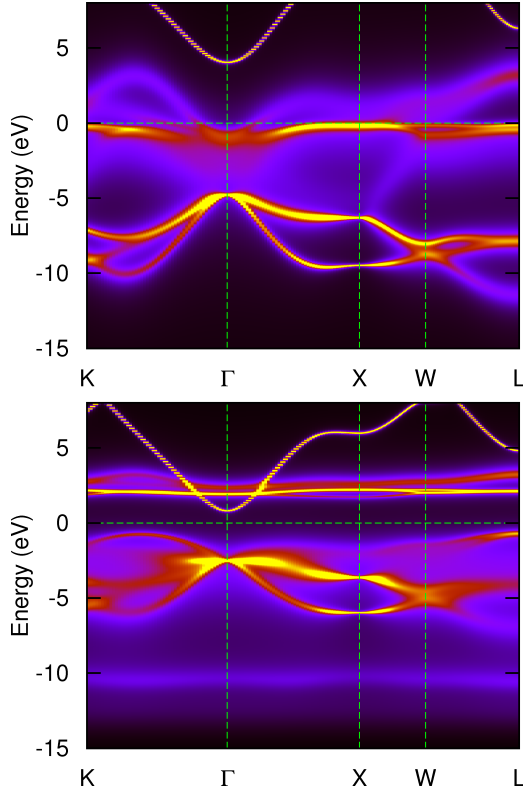


FIG. 3: The \mathbf{k} -resolved spectral function of paramagnetic FeO computed within GGA+DMFT for different volumes. Top: Results for the LS phase with lattice volume $\nu \sim 0.6$. Bottom: The equilibrium HS phase.

-4 eV below the Fermi level, but still have a substantial contribution near the Fermi level. We note however that the Fe t_{2g} states are seen to have a predominant contribution around the Fermi level. We therefore interpret paramagnetic FeO as a Mott-Hubbard insulator, in agreement with previous studies. Furthermore, our calculations show an entire reconstruction of the electronic structure of paramagnetic FeO in the LS phase [see Fig. 3 (top)]. Namely, we obtain a strongly correlated metal with almost completely occupied t_{2g} band, which is located in the vicinity of the Fermi level, and a broad disperse spectral weight originating from the Fe e_g band crossing the Fermi level. Moreover, the Fe t_{2g} states exhibit a resonant state just below the Fermi level which can be ascribed to the Zhang-Rice bound state. The O $2p$ states are shifted to about -8 eV below the Fermi level, and now have a moderate contribution near the Fermi level.

We also calculate the local (dynamical) spin-spin correlation function $\chi(\tau) = \langle \hat{m}_z(\tau) \hat{m}_z(0) \rangle$ of paramagnetic FeO for different volumes, where τ is the imaginary time. In Fig. 4 we display our results for the corresponding intra-orbital t_{2g} and e_g contributions. We note that the t_{2g} contributions are seen to be almost independent of τ , even in the LS state, implying that the t_{2g} moment remains localized across the HS-LS transition. On the

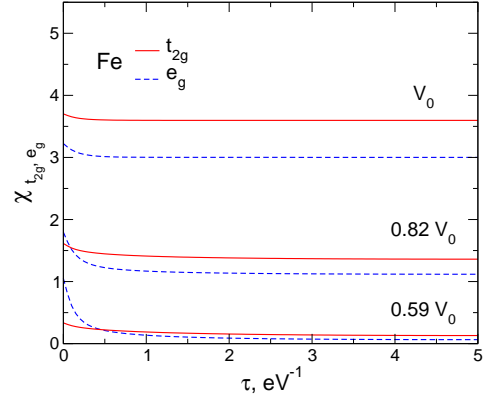


FIG. 4: Local spin-spin correlation function $\chi(\tau)$ calculated by GGA+DMFT for paramagnetic FeO as a function of volume. The intra-orbital t_{2g} and e_g contributions are shown.

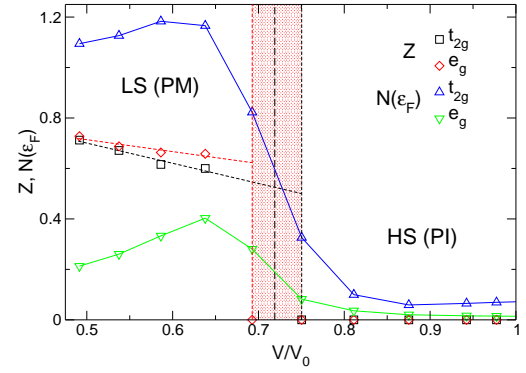


FIG. 5: Quasiparticle weight Z and spectral weight at the Fermi level $N(\epsilon_F) = -\frac{\beta}{\pi} G(\tau = \beta/2)$ calculated for the Fe t_{2g} and e_g orbitals across the MIT in paramagnetic FeO. The structural change associated with the HS-LS transition is indicated by a vertical black dashed line. The orbital-selective MIT phase is marked by a red filled rectangle.

other hand, the e_g states clearly exhibit a crossover from localized to itinerant magnetic behavior under pressure, suggesting that the HS-LS metal-insulator transition in paramagnetic FeO is of the orbital-selective type. In addition, we notice that at high pressures the screened local moment defined as $\propto \int_0^{1/T} d\tau \chi(\tau)$ differs from the corresponding instantaneous $\langle m_z^2 \rangle$ value (mostly because of the contribution originating from the e_g band), which suggests an itinerant-moment behavior of the LS state.

Finally, we calculate the quasiparticle weight employing a polynomial fit of the imaginary part of the self-energy $\Sigma(i\omega_n)$ at the lowest Matsubara frequencies ω_n . It is evaluated as $Z = [1 - \partial \text{Im} \Sigma(i\omega) / \partial i\omega]^{-1}$ from the slope of the polynomial fit at $\omega = 0$. In Fig. 5 we present our results for the partial t_{2g} and e_g contributions computed for different volumes. In the LS phase, the t_{2g} and e_g quasiparticle weights are finite and found to decrease monotonously upon expansion of the lattice. Upon further expansion of the lattice, the t_{2g} and e_g Z factors are seen to collapse to zero at different volumes. This result

again suggests that the HS-LS transition is accompanied by an orbital-selective MIT. The electronic effective mass diverges at the MIT, in accordance with a Brinkman-Rice picture of the MIT.⁴⁷ We note that this divergence coincides with the drop of the spectral weight for the t_{2g} and e_g orbitals at the Fermi level shown in Fig. 5.

IV. CONCLUSION

We determined the electronic structure and phase stability of the B1 crystal structure of paramagnetic FeO at high pressure and temperature. Our results clearly establish a high-spin to low-spin transition which is found to appear upon compression of the lattice by $V/V_0 \sim 0.72$, at pressure 73 GPa, in agreement with experiment. The spin-state transition is intimately linked with an orbital-selective Mott-Hubbard metal-insulator transition. The

MIT is accompanied by a collapse of the lattice volume by $\sim 8.5\%$, implying a complex interplay between electronic and lattice degrees of freedom. Upon compression, the Fe e_g states exhibit a crossover from a localized to itinerant-moment behavior, while the t_{2g} moment remains localized across the HS-LS transition. Our results are consistent with the picture of an electronically driven spin-state transition and volume collapse in the B1 crystal structure of paramagnetic FeO.

Acknowledgments

We thank V. I. Anisimov, and D. Vollhardt for valuable discussions. Support by the Deutsche Forschungsgemeinschaft through Transregio TRR 80 is gratefully acknowledged.

-
- ¹ H. Mao, J. Shu, Y. Fei, J. Hu, and R. J. Hemley, *Phys. Earth Planet. Inter.* **96**, 135 (1996); R. A. Fischer, A. J. Campbell, O. T. Lord, G. A. Shofner, P. Dera, and V. B. Prakapenka, *Geophys. Res. Lett.* **38**, L24301 (2011); R. A. Fischer, A. J. Campbell, G. A. Shofner, O. T. Lord, P. Dera, V. B. Prakapenka, *Earth Planet. Sci. Lett.* **304**, 496 (2011); K. Ohta, K. Fujino, Y. Kuwayama, T. Kondo, K. Shimizu, and Y. Ohishi, *J. Geophys. Res. Solid Earth*, **119**, doi:10.1002/2014JB010972.
 - ² C. A. McCammon, *J. Magn. Magn. Mater.* **104**, 1937 (1992); A. P. Kantor, S. D. Jacobsen, I. Yu. Kantor, L. S. Dubrovinsky, C. A. McCammon, H. J. Reichmann, and I. N. Goncharenko, *Phys. Rev. Lett.* **93**, 215502 (2004).
 - ³ B. T. M. Willis and H. P. Rooksby, *Acta Crystallogr.* **6**, 827 (1953). C. A. McCammon and L. Liu, *Phys. Chem. Miner.* **10**, 106 (1984); T. Yagi, T. Suzuki, and S. Akimoto, *J. Geophys. Res.* **90**, 8784 (1985). S. Ono, Y. Ohishi, and T. Kikegawa, *J. Phys. Condens. Matter* **19**, 036205 (2007).
 - ⁴ Y. Fei and H.-K. Mao, *Science* **266**, 1678 (1994); K. Ohta, K. Hirose, K. Shimizu, and Y. Ohishi, *Phys. Rev. B* **82**, 174120 (2010); H. Ozawa, K. Hirose, S. Tatenos, N. Sata, and Y. Ohishi, *Phys. Earth Planet. Inter.* **179**, 157 (2010);
 - ⁵ H. Ozawa, K. Hirose, K. Ohta, H. Ishii, N. Hiraoka, Y. Ohishi, and Y. Seto, *Phys. Rev. B* **84**, 134417 (2011).
 - ⁶ D. G. Isaak, R. E. Cohen, M. J. Mehl, and D. J. Singh, *Phys. Rev. B* **47**, 7720 (1993). R. E. Cohen, I. I. Mazin, and D. G. Isaak, *Science* **275**, 654 (1997).
 - ⁷ I. I. Mazin and V. I. Anisimov, *Phys. Rev. B* **55**, 12822 (1997).
 - ⁸ I. I. Mazin, Y. Fei, R. Downs, and R. Cohen, *Amer. Mineral.* **83**, 451 (1998).
 - ⁹ Z. Fang, K. Terakura, H. Sawada, T. Miyazaki, and I. Solovyev, *Phys. Rev. Lett.* **81**, 1027 (1998); Z. Fang, I. V. Solovyev, H. Sawada, and K. Terakura, *Phys. Rev. B* **59**, 762 (1999).
 - ¹⁰ S. A. Gramsch, R. E. Cohen, and S. Yu. Savrasov, *Amer. Mineral.* **88**, 257 (2003).
 - ¹¹ F. Tran, P. Blaha, K. Schwarz, and P. Novák, *Phys. Rev. B* **74**, 155108 (2006).
 - ¹² J. Koloenc and L. Mitas, *Phys. Rev. Lett.* **101**, 185502 (2008).
 - ¹³ A. O. Shorikov, Z. V. Pchelkina, V. I. Anisimov, S. L. Skornyakov, and M. A. Korotin, *Phys. Rev. B* **82**, 195101 (2010).
 - ¹⁴ K. Ohta, R. E. Cohen, K. Hirose, K. Haule, K. Shimizu, and Y. Ohishi, *Phys. Rev. Lett.* **108**, 026403 (2012).
 - ¹⁵ E. Holmström and L. Stixrude, *Phys. Rev. Lett.* **114**, 117202 (2015).
 - ¹⁶ E. Knittle, R. Jeanloz, A. C. Mitchell, and W. J. Nellis, *Solid State Commun.* **59**, 513 (1986).
 - ¹⁷ M. P. Pasternak, R. D. Taylor, R. Jeanloz, X. Li, J. H. Nguyen, and C. A. McCammon, *Phys. Rev. Lett.* **79**, 5046 (1997).
 - ¹⁸ J. Badro, V. V. Struzhkin, J. Shu, R. J. Hemley, H.-k. Mao, C.-C. Kao, J.-P. Rueff, and G. Shen, *Phys. Rev. Lett.* **83**, 4101 (1999).
 - ¹⁹ A. Mattila, J.-P. Rueff, J. Badro, G. Vankó, and A. Shukla, *Phys. Rev. Lett.* **98**, 196404 (2007).
 - ²⁰ R. A. Fischer and A. J. Campbell, *Am. Mineral.* **95**, 1473 (2010).
 - ²¹ W. Metzner and D. Vollhardt, *Phys. Rev. Lett.* **62**, 324 (1989); A. Georges, G. Kotliar, W. Krauth, and M. J. Rozenberg, *Rev. Mod. Phys.* **68**, 13 (1996); G. Kotliar and D. Vollhardt, *Phys. Today* **57**(3), 53 (2004).
 - ²² V. I. Anisimov, A. I. Poteryaev, M. A. Korotin, A. O. Anokhin, and G. Kotliar, *J. Phys. Condens. Matter* **9**, 7359 (1997); A. I. Lichtenstein and M. I. Katsnelson, *Phys. Rev. B* **57**, 6884 (1998); G. Kotliar, S. Y. Savrasov, K. Haule, V. S. Oudovenko, O. Parcollet, and C. A. Marianetti, *Rev. Mod. Phys.* **78**, 865 (2006).
 - ²³ S. Y. Savrasov, G. Kotliar, and E. Abrahams, *Nature* **410**, 793 (2001); X. Dai, S. Y. Savrasov, G. Kotliar, A. Migliori, H. Ledbetter, and E. Abrahams, *Science* **9**, 953, (2003).
 - ²⁴ K. Held, G. Keller, V. Eyert, D. Vollhardt, and V. I. Anisimov, *Phys. Rev. Lett.* **86**, 5345 (2001); G. Keller, K. Held, V. Eyert, D. Vollhardt, and V. I. Anisimov, *Phys. Rev. B* **70**, 205116 (2004).
 - ²⁵ K. Held, A. K. McMahan, and R. T. Scalettar, *Phys. Rev. Lett.* **87**, 276404 (2001); A. K. McMahan, K. Held, and R. T. Scalettar, *Phys. Rev. B* **67**, 075108 (2003).

- ²⁶ S. Y. Savrasov, K. Haule, and G. Kotliar, Phys. Rev. Lett. **96**, 036404 (2006).
- ²⁷ B. Amadon, S. Biermann, A. Georges, and F. Aryasetiawan, Phys. Rev. Lett. **96**, 066402 (2006); N. Lanatá, Y.-X. Yao, C.-Z. Wang, K.-M. Ho, J. Schmalian, K. Haule, and G. Kotliar, Phys. Rev. Lett. **111**, 196801 (2013); J. Bieder and B. Amadon, Phys. Rev. B **89**, 195132 (2014); B. Chakrabarti, M. E. Pezzoli, G. Sordi, K. Haule, and G. Kotliar, Phys. Rev. B **89**, 125113 (2014).
- ²⁸ J. Kunes, V. I. Anisimov, A. V. Lukoyanov, and D. Vollhardt, Phys. Rev. B **75**, 165115 (2007); J. Kunes, V. I. Anisimov, S. L. Skornyakov, A. V. Lukoyanov, and D. Vollhardt, Phys. Rev. Lett. **99**, 156404 (2007).
- ²⁹ I. Leonov, N. Binggeli, D. Korotin, V. I. Anisimov, N. Stojić, and D. Vollhardt, Phys. Rev. Lett. **101**, 096405 (2008); I. Leonov, Dm. Korotin, N. Binggeli, V. I. Anisimov, and D. Vollhardt, Phys. Rev. B **81**, 075109 (2010); J. Kunes, I. Leonov, M. Kollar, K. Byczuk, V. I. Anisimov, D. Vollhardt, Eur. Phys. J. Spec. Top. **180**, 5 (2010).
- ³⁰ J. Kunes, A. V. Lukoyanov, V. I. Anisimov, R. T. Scalettar, and W. E. Pickett, Nat. Mater. **7**, 198 (2008); J. Kunes, Dm. M. Korotin, M. A. Korotin, V. I. Anisimov, and P. Werner, Phys. Rev. Lett. **102**, 146402 (2009).
- ³¹ I. Di Marco, J. Minár, S. Chadov, M. I. Katsnelson, H. Ebert, and A. I. Lichtenstein, Phys. Rev. B **79**, 115111 (2009).
- ³² I. Leonov, A. I. Poteryaev, V. I. Anisimov, and D. Vollhardt, Phys. Rev. Lett. **106**, 106405 (2011); I. Leonov, A. I. Poteryaev, V. I. Anisimov, and D. Vollhardt, Phys. Rev. B **85**, 020401(R) (2012); I. Leonov, A. I. Poteryaev, Yu. N. Gornostyrev, A. I. Lichtenstein, M. I. Katsnelson, V. I. Anisimov, D. Vollhardt, Sci. Rep. **4**, 5585 (2014).
- ³³ M. Aichhorn, L. Pourovskii, and A. Georges, Phys. Rev. B **84**, 054529 (2011).
- ³⁴ L. Huang, Y. Wang, and X. Dai, Phys. Rev. B **85**, 245110 (2012); A. A. Dyachenko, A. O. Shorikov, A. V. Lukoyanov, and V. I. Anisimov, JETP Lett. **96**, 56 (2012).
- ³⁵ D. Grieger, C. Piefke, O. E. Peil, and F. Lechermann, Phys. Rev. B **86**, 155121 (2012); D. Grieger and F. Lechermann, *ibid.* **90**, 115115 (2014); I. Leonov, V. I. Anisimov, and D. Vollhardt, Phys. Rev. B **91**, 195115 (2015).
- ³⁶ H. Park, A. J. Millis, C. A. Marianetti, Phys. Rev. B **89**, 245133 (2014).
- ³⁷ K. Glazyrin, L. V. Pourovskii, L. Dubrovinsky, O. Narygina, C. McCammon, B. Hewener, V. Schünemann, J. Wolny, K. Muffler, A. I. Chumakov, W. Crichton, M. Hanfland, V. B. Prakapenka, F. Tasnadi, M. Ekholm, M. Aichhorn, V. Vildosola, A. V. Ruban, M. I. Katsnelson, and I. A. Abrikosov, Phys. Rev. Lett. **110**, 117206 (2013); L. V. Pourovskii, J. Mravlje, M. Ferrero, O. Parcollet, and I. A. Abrikosov, Phys. Rev. B **90**, 155120 (2014).
- ³⁸ I. Leonov, V. I. Anisimov, and D. Vollhardt, Phys. Rev. Lett. **112**, 146401 (2014).
- ³⁹ For a review, see, e.g., L. V. Pourovskii, B. Amadon, S. Biermann, and A. Georges, Phys. Rev. B **76**, 235101 (2007); K. Haule, *ibid.* **75**, 155113 (2007); B. Amadon, F. Lechermann, A. Georges, F. Jollet, T. O. Wehling, and A. I. Lichtenstein, *ibid.* **77**, 205112 (2008); M. Aichhorn, L. Pourovskii, V. Vildosola, M. Ferrero, O. Parcollet, T. Miyake, A. Georges, and S. Biermann, *ibid.* **80**, 085101 (2009); B. Amadon, J. Phys. Condens. Matter **24**, 075604 (2012); H. Park, A. J. Millis, and C. A. Marianetti, Phys. Rev. B **90**, 235103 (2014).
- ⁴⁰ S. Baroni, S. de Gironcoli, A. Dal Corso, and P. Giannozzi, Rev. Mod. Phys. **73**, 515 (2001); P. Giannozzi, S. Baroni, N. Bonini, M. Calandra, R. Car *et al.*, J. Phys. Condens. Matter **21**, 395502 (2009).
- ⁴¹ N. Marzari and D. Vanderbilt, Phys. Rev. B **56**, 12847 (1997); N. Marzari, A. A. Mostofi, J. R. Yates, I. Souza, and D. Vanderbilt, Rev. Mod. Phys. **84**, 1419 (2012).
- ⁴² V. I. Anisimov, D. E. Kondakov, A. V. Kozhevnikov, I. A. Nekrasov, Z. V. Pchelkina, J. W. Allen, S.-K. Mo, H.-D. Kim, P. Metcalf, S. Suga, A. Sekiyama, G. Keller, I. Leonov, X. Ren, and D. Vollhardt, Phys. Rev. B **71**, 125119 (2005); G. Trimarchi, I. Leonov, N. Binggeli, Dm. Korotin, and V. I. Anisimov, J. Phys. Condens. Matter **20**, 135227 (2008); Dm. Korotin, A. V. Kozhevnikov, S. L. Skornyakov, I. Leonov, N. Binggeli, V. I. Anisimov and G. Trimarchi, Eur. Phys. J. B **65**, 91 (2008).
- ⁴³ P. Werner, A. Comanac, L. de'Medici, M. Troyer, and A. J. Millis, Phys. Rev. Lett. **97**, 076405 (2006); E. Gull, A. J. Millis, A. I. Lichtenstein, A. N. Rubtsov, M. Troyer, and P. Werner, Rev. Mod. Phys. **83**, 349 (2011).
- ⁴⁴ P. S. Bagus, C. R. Brundle, T. J. Chuang, and K. Wandelt, Phys. Rev. Lett. **39**, 1229 (1977); I. Balberg and H. L. Pinch, J. Magn. Magn. Mater. **7**, 12 (1978).
- ⁴⁵ F. D. Murnaghan, Proc. Natl. Acad. Sci. U.S.A. **30**, 244 (1944); F. Birch, Phys. Rev. **71**, 809 (1947).
- ⁴⁶ F. C. Zhang and T. M. Rice, Phys. Rev. B **37**, 3759(R) (1988); J. Bala, A. M. Oleś, and J. Zaanen, Phys. Rev. Lett. **72**, 2600 (1994); Q. Yin, A. Gordienko, X. Wan, and S. Y. Savrasov, *ibid.* **100**, 066406 (2008).
- ⁴⁷ W. F. Brinkman and T. M. Rice, Phys. Rev. B **2**, 4302 (1970).